Supramolecular Chemistry
Publication details, including instructions for authors and subscription information:
http://www.informaworld.com/smpp/title~content=t713649759

Inclusion complex of riboflavin with cucurbit[7]uril: study in solution and solid state

Yunyou Zhou[a]; Junyong Sun[a]; Huapeng Yu[a]; Lian Wu[a]; Lun Wang[a]
[a] Anhui Key Laboratory of Functional Molecular Solids, College of Chemistry and Materials Science, Anhui Normal University, Wuhu, P.R. China

To cite this Article Zhou, Yunyou , Sun, Junyong , Yu, Huapeng , Wu, Lian and Wang, Lun(2009) 'Inclusion complex of riboflavin with cucurbit[7]uril: study in solution and solid state', Supramolecular Chemistry, 21: 6, 495 — 501
To link to this Article: DOI: 10.1080/10610270802406553
URL: http://dx.doi.org/10.1080/10610270802406553

Supramolecular Chemistry
Vol. 21, No. 6, September 2009, 495–501

Taylor & Francis
Taylor & Francis Group

Inclusion complex of riboflavin with cucurbit[7]uril: study in solution and solid state

Yunyou Zhou*, Junyong Sun, Huapeng Yu, Lian Wu and Lun Wang

Anhui Key Laboratory of Functional Molecular Solids, College of Chemistry and Materials Science, Anhui Normal University, Wuhu, P.R. China

(*Received 17 January 2008; final version received 13 August 2008*)

The aqueous solution of riboflavin and cucurbit[7]uril complex has been studied based on fluorescence and ^{1}H NMR spectroscopic results. Upon addition of cucurbit[7]uril, the fluorescence intensity of riboflavin was quenched and a slight red shift was observed for the maximum emission peak. These results indicated that the cucurbit[7]uril–riboflavin complex was formed at a 1:1 mole ratio. The temperature-dependent inclusion constants were calculated, from which ΔH and ΔS values were calculated. Meanwhile, rationale of the interaction mechanism was also discussed based on ^{1}H NMR results. The solid inclusion complex was prepared from co-evaporation method and characterised by differential thermal analysis and fluorescence lifetime analysis methods. The experimental results indicated that riboflavin and cucurbit[7]uril formed stable host–guest inclusion complex in both solution and solid states.

Keywords: cucurbit[7]uril; riboflavin; fluorescence; inclusion interaction; thermodynamics

Introduction

Vitamins are a diverse group of compounds that widely exist in many biomolecules. Although they played key roles in maintaining human healthy, usually relatively small amounts were required for their proper functions. Among those, flavins, a general name for those compounds that contain a heterocyclic isoalloxazine chromophore, are cofactors involved in many biological processes that are essential for maintaining the living conditions of organisms (*1*). Among those, riboflavin (vitamin B_2, Figure 1) is the most common one, which acts as the co-enzyme precursor of flavoproteins presented in all organisms (*2*, *3*). Deficiency of vitamin B_2 has been linked to cancer, cardiovascular disease, anaemia, and various neurological and developmental disorders in humans and experimental animals (*4*). Thus, it has been widely studied in yeast, bacteria and organisms (*5*) and as a blue-light absorbing dye with rich redox chemistry and photochemistry (*6*).

Cucurbiturils as the fourth generation of host molecules have a highly symmetrical structure similar to cyclodextrins (*7*) and calixarenes (*8*). In the last few years, they have attracted much more attraction in understanding the properties of cucurbit[n]urils (*9–11*). Among those, many fundamental studies have been performed in studying the related host–guest inclusion complexes (*12*, *13*). However, few investigations of the inclusion mechanism has been reported. Thus, the fundamental investigation of cucurbit[n]urils and its properties is still essential at present.

Herein, we studied the inclusion behaviour of cucurbit[7]uril (CB7, Figure 1) with riboflavin (vitamin B_2, VB2) in both solution and solid states. Our investigation would be very helpful for further understanding cucurbit[n]urils and extending their applications in the biochemistry area.

Experimental

Materials

Cucurbit[7]uril was synthesised according to the modified procedure (*14–16*) and was identified by IR and ^{1}H NMR. Stock solutions of CB7 were prepared at 1.00×10^{-3} mol L^{-1} concentration. Riboflavin (>98%) was obtained from Shanghai Chemical Reagent Co. (Shanghai, China). Its aqueous stock solution was prepared at 1.00×10^{-4} mol L^{-1} concentration. All the working solutions were prepared by diluting the stock solutions to the required concentrations. Deuterium oxide (99.9%) was purchased from Acros Co. (Andover Massachusetts, USA). Doubly distilled water was used thoroughly.

Apparatus

Fluorescence spectra and relative fluorescence intensities were measured on a model F-4500 fluorescence

*Corresponding author. Email: zy161299@mail.ahnu.edu.cn

ISSN 1061-0278 print/ISSN 1029-0478 online

DOI: 10.1080/10610270802406553
http://www.informaworld.com

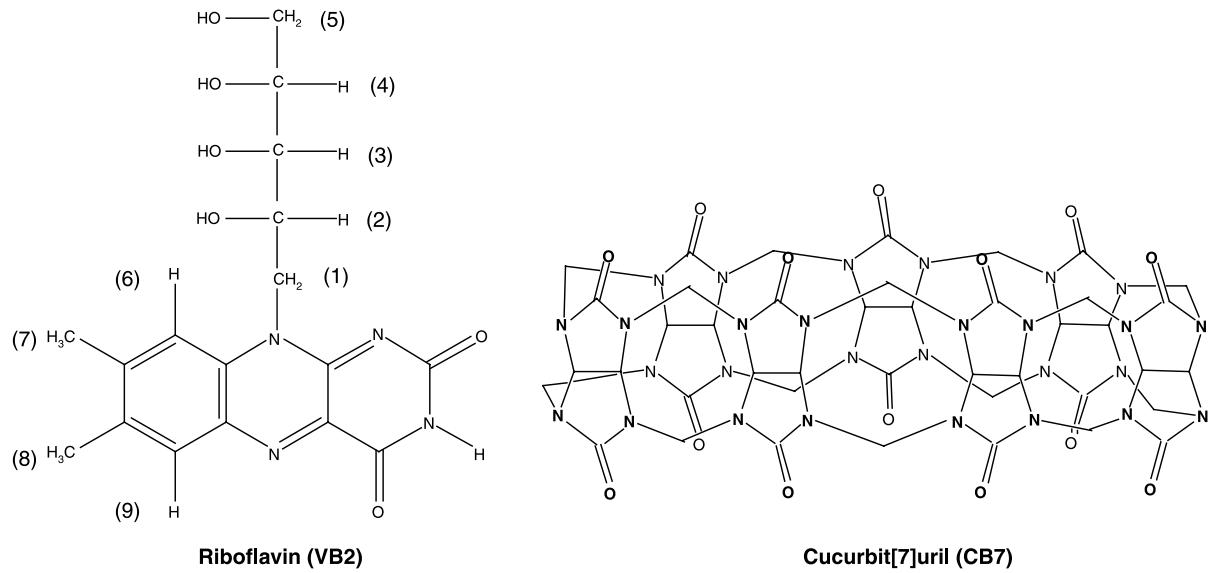

Figure 1. Molecular structures of fluorescent guest molecule riboflavin (VB2) and the host molecule cucurbit[7]uril (CB7).

spectrophotometer (Hitachi, Japan) using a conventional 1 cm × 1 cm quartz cell. Excitation and emission bandwidths were set to 5 nm. All the measurements were carried out at desired temperature using a thermostatic cell holder. A pHS-3C meter (Dazhong Analytical Instruments Factory, Shanghai, China) was used for accurate adjustment of pH. ^{1}H NMR spectra were measured using an Avance Bruker-400 MHz spectrometer. Thermal analyses were performed on a Shimadzu DTG-60A simultaneous DTA-TG apparatus (Toyota, Japan). The fluorescence lifetimes were measured on a FLS920 combined steady-state lifetime fluorescence spectrometer (Edinburgh Instrument).

Methods

To a 10 ml volumetric flask was added 0.5 ml VB2 stock solution (1.00×10^{-4} mol L^{-1}) and a specific amount of CB7 solution (1.00×10^{-3} mol L^{-1}). Then the mixture was diluted to the final volume with water and was left stirring thoroughly. After stirring for 15 min at appropriate temperature, fluorescence intensities test was performed.

All NMR spectra were collected in D_2O. First, VB2 was dissolved in D_2O to generate its saturated solution (around 6.24×10^{-4} mol L^{-1}). To this saturated VB2 solution was added CB7 powder and the mixture solution of VB2 and CB7 was obtained.

The solid complex of VB2 with CB7 at 1:1 molar ratio, used for differential thermal analysis (DTA), and fluorescence lifetime measurements, was prepared from co-evaporation. First, at 80°C, VB2 (20.0 mg) was dissolved in 50 ml 3% acetic acid aqueous solution and was left stirring for 30 min to generate a homogeneous solution. Then CB7 aqueous solution, prepared by dissolving CB7 (58.1 mg) in distilled water, was slowly added to this solution. The resulting mixture was left stirring for 4 h at 80°C before removing solvent to generate fine powder. This fine powder was then washed with acetone. Finally, acetone was removed under vacuum at 50°C and the final product was pulverised, from which the mixture of VB2 and CB7 at 1:1 molar ratio was obtained.

Results and discussion

The aqueous solution of VB2 has strong fluorescence at pH 7, with the maximum excitation and emission peaks correspondingly at 460 nm and 537 nm. With addition of CB7 (1.00×10^{-3} mol L^{-1}), the fluorescence intensity of

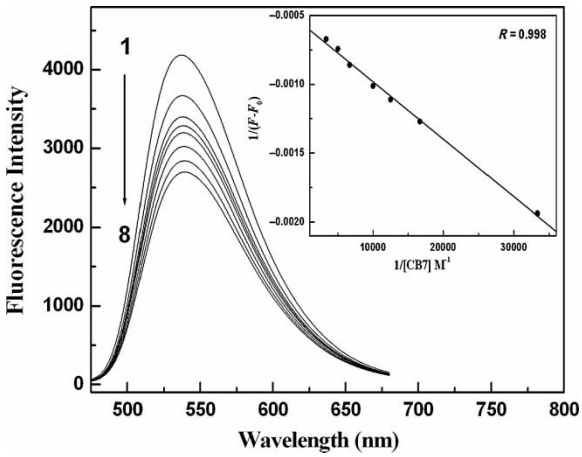

Figure 2. Fluorescence spectra of VB2 (5.00×10^{-6} mol L^{-1}) with addition of CB7. The concentration of CB7 that varies from (1) to (8) is (1) 0, (2) 30, (3) 60, (4) 80, (5) 100, (6) 150, (7) 200 and (8) 300×10^{-6} mol L^{-1}.

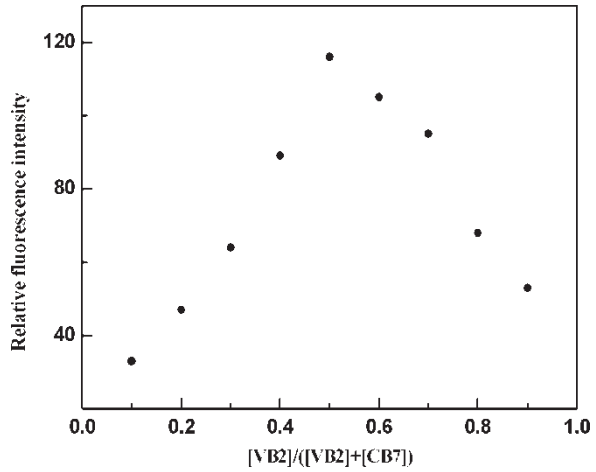

Figure 3. Job's plot for the CB7–VB2 complex, with the mole fraction of VB2, varies from 0.1 to 0.9.

VB2 decreased dramatically, together with a small red shift of the maximum emission peak (see Figure 2). This fluorescence changes indicated the formation of the inclusion complexes. To study the suitable condition for the inclusion interaction, we first studied pH effect in forming the VB2–CB7 inclusion complex. In acidic and alkaline solutions, the interaction between VB2 and CB7 can hardly be observed from the change of fluorescence. The inclusion phenomenon is weak. From our point of view, the strong influence from pH might come from the different conformation of VB2 at various conditions (cationic, neutral and anionic riboflavin species in aqueous solution) (*17*). Since VB2 has interacted with CB7 through the neutral species conformation. Therefore, the cationic (in acidic solution) and anionic riboflavin species (at alkaline solution) have small interaction with CB7.

The stoichiometry and inclusion constant of the inclusion complex were studied under the established

Table 1. Inclusion constants of complexes at different temperatures.

Temperature (T/K)	Inclusion constants ($K/10^4 M^{-1}$)
293	1.35 ± 0.05
298	1.25 ± 0.06
305	0.96 ± 0.05
313	0.76 ± 0.04
325	0.47 ± 0.05

experimental conditions, and the following expression was derived:

$$\frac{1}{F - F_0} = \frac{1}{(F_1 - F_0)} + \frac{1}{K[H](F_1 - F_0)}. \qquad (1)$$

Here, we made an assumption that the complex consists of VB2 and CB7 at 1:1 molar ratio. A similar equation has already been proposed in the cyclodextrin system by Mwalupindi *et al.* (*18*) and Singh *et al.* (*19*). Here, the guest molecule is VB2 and the host molecule is CB7. In this equation, F refers to the fluorescence intensity of the host molecule at various concentrations, F_0 refers to the fluorescence intensity of VB2 at the absence of CB7, and F_1 refers to the fluorescence intensity at the presence of CB7. The double reciprocal plots (Benesi–Hilderbrand plots) of $1/(F - F_0)$ versus 1/[CB7] given in the inset of Figure 2 show linear relations ($R = 0.998$), which confirmed the formation of a 1:1 stoichiometry between CB7 and VB2. The inclusion constant of the complex can be estimated from the ratio of intercept to slope, which is $1.35 \times 10^4\,\mathrm{L\,mol^{-1}}$ at 293 K. Although the double-reciprocal linear approach of Benesi–Hilderbrand plots had been well known for the over-emphasis of the data at a low host-concentration, it was still suitable for our system when considering the host concentration is ten times larger than the guest in our experiment condition.

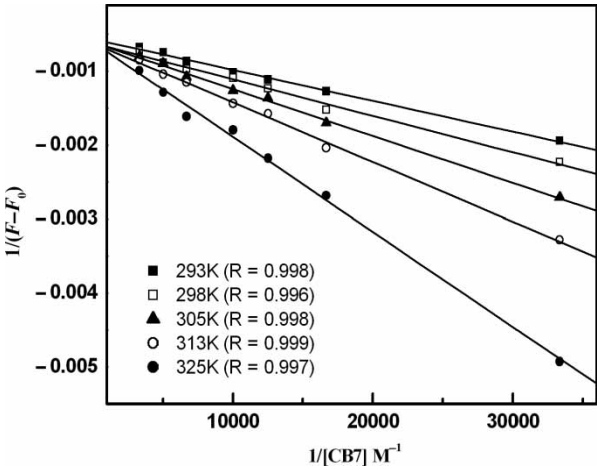

Figure 4. Benesi–Hilderbrand plots for 1:1 VB2–CB7 complex at various temperatures.

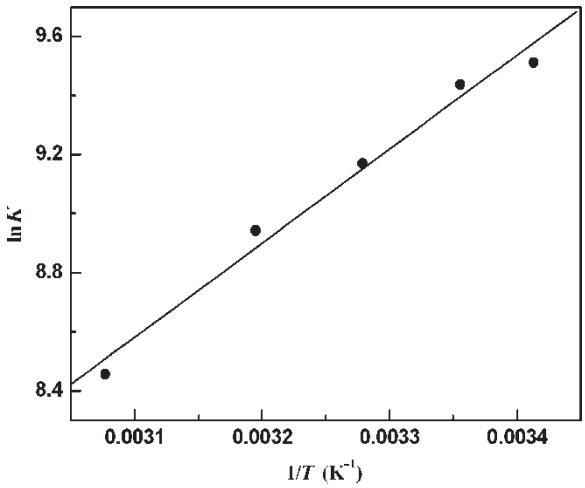

Figure 5. The plot of ln$K$ versus $1/T$ for the VB2–CB7 complex.

This 1:1 stoichiometry inclusion complexes were also confirmed by the continuous variation method (Job's plot) using fluorescence results. Here, VB2 and CB7 were mixed in various mole ratios, while keeping the total concentration of the mixture and host concentration to be constant. Figure 3 shows symmetric relative fluorescence intensity changes with the maximum one corresponding to 0.5 mole fractions of [VB2], which is in agreement with the above Benesi–Hilderbrand plot results and confirmed the formation of a 1:1 inclusion complex in the system.

The thermodynamics parameters (changes in enthalpy, entropy and Gibbs energy) for the inclusion reaction were obtained from the temperature-dependent fluorescence spectra data of VB2 at the presence of CB7. The double reciprocal plot in Figure 4 was collected at various temperatures, from which the inclusion constant values

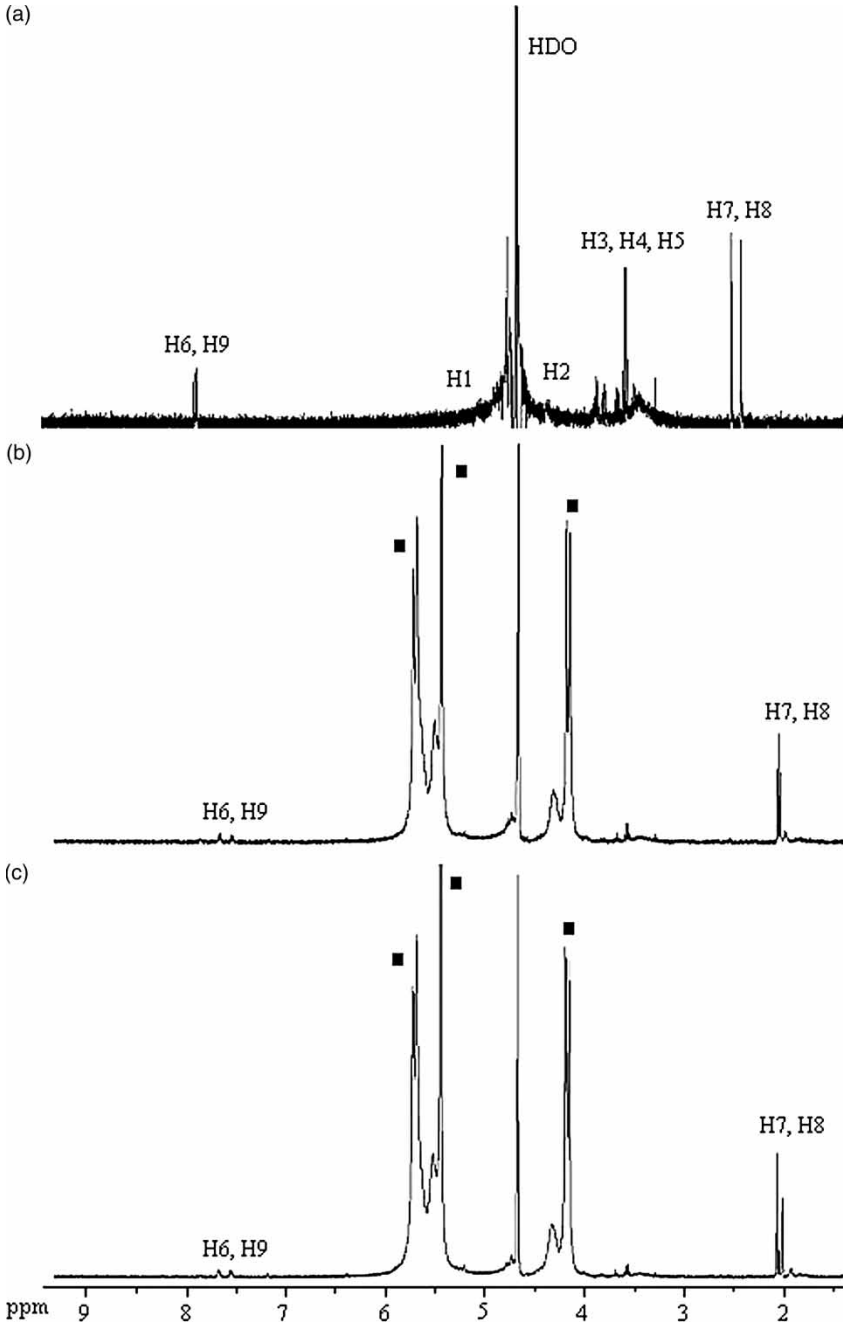

Figure 6. ^{1}H NMR spectrum changes of VB2 with the addition of CB7 (■): (a) no CB7; (b) 1 molar equivalent of CB7; (c) 5 molar equivalent of CB7.

K were obtained and summarised in Table 1. Based on the data from Table 1, the inclusion constants decreased gradually with the increasing of the temperature. The corresponding enthalpy ΔH ($-26.44\,kJ\,mol^{-1}$) and entropy ΔS ($-10.63\,J\,mol^{-1}K^{-1}$) were obtained from the classical method, by plotting ln*K* versus 1/*T* (the Van't Hoff method (*20*); Figure 5, $R = 0.9912$). These results suggested that the formation of VB2–CB7 complex was favoured when considering the enthalpic driving force. It may seem unusual for cation receptors to participate in the inclusion complex formation; however similar observations have been made for the formation of complexes between cucurbit[6]uril and several other organic cations (*21*). CB7 possesses two equivalent ureido carbonyl rims, which possess the cation-binding properties. Meanwhile, water molecules are included in the cavity of CB7 through non-hydrogen bonds form. The dipole–dipole interaction between the protonated groups of VB2 and the carbonyl groups of CB7 are an important factor in promoting the formation of the corresponding host–guest inclusion complex (*22, 23*). Meanwhile, the releasing of additional solvent molecules during the complex formation process might also be helpful for the complex formation. The negative ΔS value was due to the restrict motion of the encapsulated VB2. The relevant free energy change (ΔG) for this system is $-23.28\,kJ\,mol^{-1}$ at 298 K, which indicated the formation of VB2–CB7 complex is an energetically favoured process.

It has been reported that the fluorescence intensity of guest molecules generally increased gradually with the addition of CB7 (*12, 13, 24*). However, in our system, instead of increasing, the fluorescence intensity of VB2 decreased with the addition of the CB7. According to the Benesi–Hilderbrand plot, the fluorescence quenching might be induced by the formation of CB7–VB2 complex. This fluorescence quenching behaviour was similar to the β-cyclodextrin–phenolphthalein inclusion complex (*25, 26*) and β-cyclodextrin–rhodamine B analogues (*27*). Here, the oxidated form of VB2 (*17*) formed a complex with CB7 via flavin group, which caused the fluorescence quenching result. This also explained the small red shift of VB2 with the addition of CB7. Further investigation is under way in our group.

The interaction between VB2 and CB7 were studied based on ^{1}H NMR results shown in Figure 6. There was a significant change of the signal patterns with variation of CB7 concentration. Initially, the resonances corresponding to the H6–H9 protons of VB2 were broadened and significantly shifted upfield upon the formation of VB2–CB7 complex (Figure 6(b,c)). Meanwhile, the resonances of H1–H5 of VB2 remain unchanged. This proton signal shift is characteristic when these protons were involved in the hydrophobic interactions with CB7 (*21*, *28*). Thus, VB2 interacted with the cavity of CB7 via encapsulation of the flavin group. Meanwhile, we have provided the quantum-mechanical molecular model to rationale

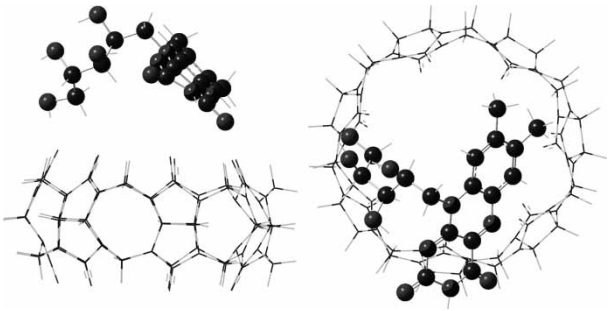

Figure 7. The quantum-mechanical molecular model for CB7 and VB2.

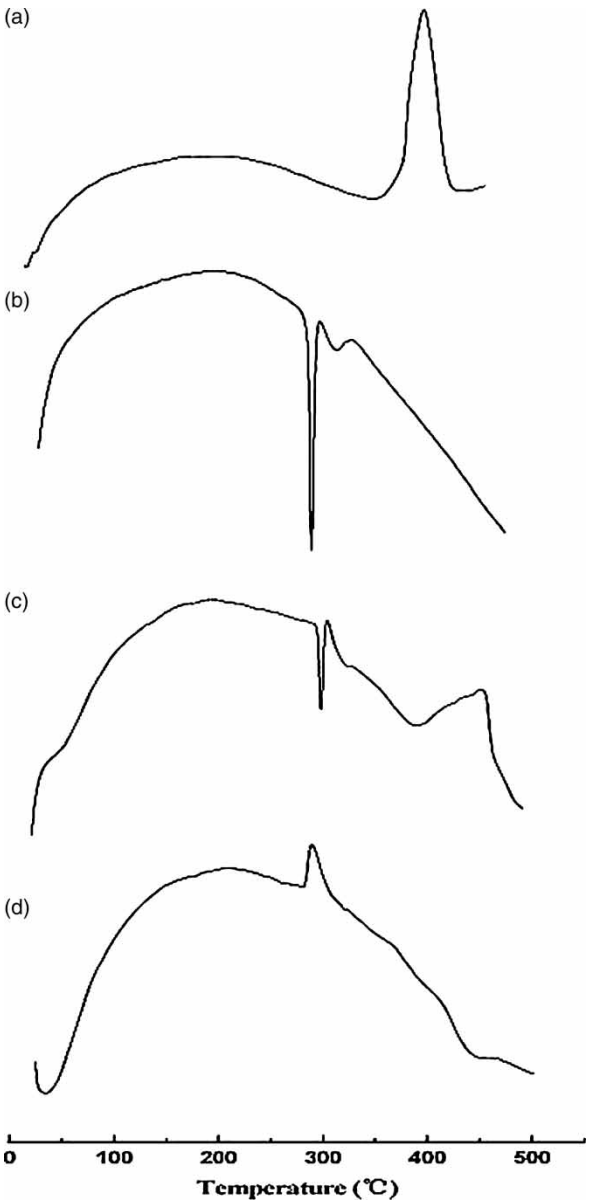

Figure 8. DTA thermograms of (a) CB7; (b) VB2; (c) VB2–CB7 physical mixture and (d) VB2–CB7 solid complex with 1:1 mole ratio.

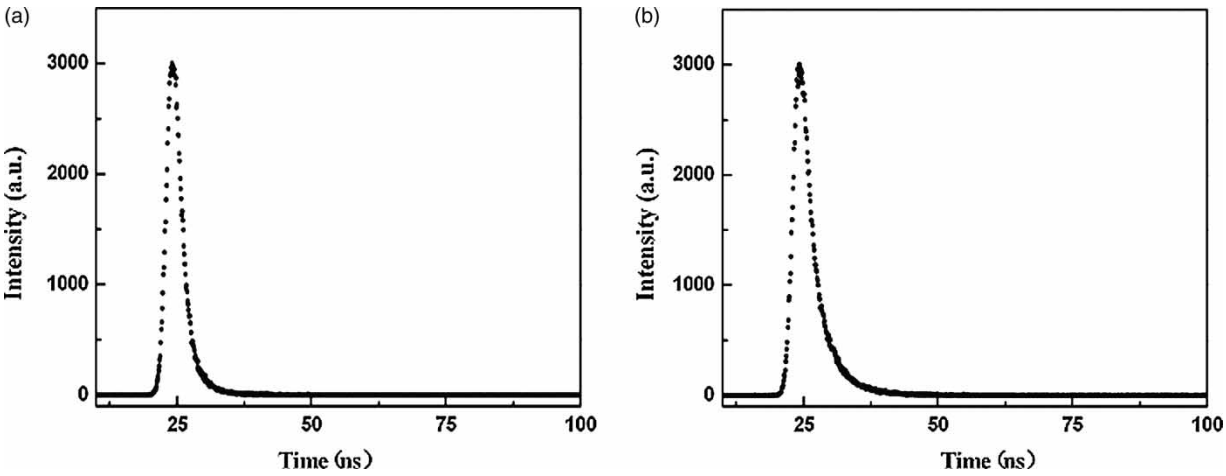

Figure 9. Fluorescence decay curve of (a) VB2; (b) VB2–CB7 complex (1:1 mole ratio) at room temperature.

inclusion complex formation (Figure 7). In Figure 7, the inclusion pattern is consistent with the one-dimensional H NMR at a certain extent; the methyl of the flavin group has interaction with CB7.

Similar to differential scanning calorimetry, DTA is commonly used for the qualitative measurement of a true inclusion complex formation (Figure 8). Free CB7 molecule displays a wide and strong exothermic reaction effect at 439°C (Figure 8(a)), while free VB2 molecule exhibits a sharp endothermic peak at 305°C, corresponding to its melting point (Figure 8(b)). The thermogram of the mixture (Figure 8(c)) showed that the melting point of VB2 remained 305°C, while the exothermic reaction effect of CB7 increased to 461°C, which might be due to the weak inclusion reaction between CB7 and VB2. However, the thermogram of VB2–CB7 complex had a dramatic change: both the exothermic reaction peak of CB7 at 439°C and the characteristic peak of VB2 at 305°C were absent. Meanwhile, a new exothermic reaction peak at 290°C appeared. These changes indicated the formation of VB2–CB7 complex (*29*).

We also measured the fluorescence lifetime of VB2 and VB2–CB7 solid complex (1:1 molar ratio). Compared with VB2 (Figure 9(a), $\tau_1 = 1.94$ ns and $\chi^2 = 1.115$), there was an obvious change of the fluorescence lifetime with the formation of the CB7–VB2 complex (Figure 9(a), $\tau_1 = 3.07$ ns and $\chi^2 = 1.230$) The increasing fluorescence lifetime is very interesting and might be useful for extending the application of cucurbit[7]uril.

Conclusion

The interaction of riboflavin with cucurbit[7]uril has been studied by several techniques, including fluorescence spectroscopy, ^{1}H NMR spectra, DTA and fluorescence lifetime. Experimental results indicate that VB2 can form a stable 1:1 host–guest inclusion complex with CB7 in both solution and solid states. Rationale of the interaction mechanism was also presented. Similar to cyclodextrin and calixarene system, cucurbit[n]uril and its inclusion complexes might also find potential applications in pharmaceutical and biological areas.

Acknowledgements

The authors thank the financial support from the National Natural Science Foundation of P. R. China (20575001), the Education Commission Natural Science Foundation of Anhui Province (2005KJ017ZD) and the Program for Innovative Research Team of Anhui Normal University. We also greatly appreciate Dr. Jiao Lijuan for her kind help regarding English grammar.

References

(1) Miura, R. *Chem. Rec.* **2001**, *1*, 183–194.
(2) Friedrich, W. *Vitamins*; Walter de Gruyter: Berlin, 1988.
(3) Niemetz, R.; Altenschmidt, U.; Brucker, S.; Fuchs, G. *Eur. J. Biochem.* **1995**, *227*, 161–168.
(4) Powers, H.-J. *Am. J. Clin. Nutr.* **2003**, *77*, 1352–1360.
(5) Bacher, A.; Eberhardt, S.; Eisenreich, W.; Fischer, M.; Herz, S.; Illarionov, B.; Kis, K.; Richter, G. *Vitam. Horm.* **2001**, *61*, 1–49.
(6) Müller, F.; Ed. *Chemistry and Biochemistry of Flavoenzymes*; CRC Press: Boca Raton, FL, 1991–1992; Vols. 1–3.
(7) Szejtli, J.; Osa, T. *Comprehensive Supramolecular Chemistry*; Pergamon Press: Oxford, UK, 1996; Vol. 3.
(8) Shinkai, S. *Tetrahedron* **1993**, *49*, 8933–8968.
(9) Lagona, J.; Mukhopadhyay, P.; Chakrabarti, S.; Isaacs, L. *Angew. Chem. Int. Ed.* **2005**, *117*, 4922–4949.
(10) Lagona, J.; Fettinger, H.C.; Isaacs, L. *Org. Lett.* **2003**, *5*, 3745–3747.
(11) Jae, W.L.; Samal, S.; Selvapalam, N.; Kim, H.J.; Kim, K. *Acc. Chem. Res.* **2003**, *36*, 621–630.
(12) Wagner, B.D.; Stojanovic, N.; Day, A.I.; Blanch, R.J. *J. Phys. Chem. B* **2003**, *107*, 10741–10746.

(13) Mohanty, J.; Bhasikuttan, A.C.; Nau, W.M.; Pal, H. *J. Phys. Chem. B* **2006**, *110*, 5132–5238.
(14) Kim, J.; Jung, I.S.; Kim, S.Y.; Lee, E.; Kang, J.K.; Sakamoto, S.; Yamaguchi, K.; Kim, K. *J. Am. Chem. Soc.* **2000**, *122*, 540–541.
(15) Day, A.; Arnold, A.P.; Blanch, R.J.; Snushall, B. *J. Org. Chem.* **2001**, *66*, 8094–8100.
(16) Marquez, C.; Fang, H.; Nau, W.M. *IEEE Trans. Nanobiosci.* **2004**, *3*, 39–41.
(17) Drössler, P.; Holzer, W.; Penzkofer, A.; Hegemann, P. *Chem. Phys.* **2002**, *282*, 429–439.
(18) Mwalupindi, A.G.; Rideau, A.; Agbaria, R.; Warner, I.M. *Talanta* **1994**, *41*, 599–609.
(19) Singh, M.K.; Pal, H.; Koti, A.S.R.; Sapre, A.V. *J. Phys. Chem. A* **2004**, *108*, 1465–1474.
(20) Liu, Y.; Han, B.-H.; Chen, Y.T. *J. Phys. Chem. B* **2002**, *106*, 4678–4687.
(21) Saleh, N.; Al-Rawashdeh Nathir, A.F. *J. Fluoresc.* **2006**, *16*, 487–493.
(22) Buschmann, H.J.; Schollmeyer, E.; Mutihac, L. *Thermochim. Acta* **2003**, *399*, 203–208.
(23) Germain, P.; Letoffe, J.M.; Merlin, M.P.; Buschmann, H.-J. *Thermochim. Acta* **1998**, *315*, 87–92.
(24) Sindelar, V.; Cejas, M.A.; Raymo, F.M.; Kaifer, A.E. *New J. Chem.* **2005**, *29*, 280–282.
(25) Taguchi, K. *J. Am. Chem. Soc.* **1986**, *108*, 2705–2709.
(26) Yoshida, N.; Shirai, T.; Fujimoto, M. *Carbohydr. Res.* **1989**, *192*, 291–304.
(27) Liu, Y.; You, C.-C. *J. Phys. Org. Chem.* **2001**, *14*, 11–16.
(28) Yannis, L.-L.; Vassiliki, V.; Gregoriadis, G. *Int. J. Pharm.* **1996**, *144*, 225–231.
(29) Loukas, Y.-L.; Vraka, V.; Gregoriadis, G. *J. Pharm. Biomed. Anal.* **1997**, *16*, 263–268.